Syntheses and Thermal and Chemical Behaviors of Tartrate and Succinate Intercalated Zn_3Al and Zn_2Cr Layered Double Hydroxides

V. Prevot, C. Forano,* and J. P. Besse

Laboratoire des matériaux inorganiques, CNRS UPRES-A 6002, Université Blaise Pascal, 63177 Aubière Cedex, France

F. Abraham

Laboratoire de Cristallochimie et Physico-Chimie du Solide, CNRS URA 452, Ecole Nationale Supérieure de Chimie de Lille, 59652 Villeneuve d'Asq Cedex, France

Received February 2, 1998

Tartrate and succinate anions have been intercalated in Zn_3Al and Zn_2Cr LDHs. The preparations using either coprecipitation, anion exchange, or reconstruction methods are described. In the case of tartrate-containing LDH, coprecipitation and reconstruction methods have proved to be very limited to lead to pure materials due to the particular reactivity of tartrate anions. Intercalation of both anions under room-temperature conditions gives rise to expanded LDH with similar basal spacing. Moderate thermal treatments lead in all cases to a reorientation of the anions in the interlayer domains associated with an interlayer contraction occurring around 80 °C. The structural characterization, the thermal evolution, and the chemical stability of all the phases are studied by PXRD, FTIR, TGA, and DTA.

Introduction

Presently organic−inorganic hybrid materials receive considerable attention owing to their very large field of application as catalysts, catalyst supports, electrochemical sensors, or sorbents for organic pollutants. Ionic exchangers intercalated by organic entities form one type (I) of hybrid materials, according to the Sanchez classification,[1] which involve weak bonding between host lattice and guest molecules. The other type (II) of hybrid materials involve covalent bonds between the organic and inorganic partners. The latter compounds display stonger interactions between the organic and mineral partners, which ensure higher chemical and structural stabilities. They concern mainly organosilicon compounds. For the former family of hybrid compounds, the improvement of the chemical and thermal stability must involve an increase of the interactions between the organic units and the inorganic surfaces. This can be obtained by the grafting of the organic molecule onto the mineral lattice, thus transforming these compounds to hybrid type II materials. Recent developments on surface-modified inorganic layered compounds have been reported which describe grafting of aliphatic or aromatic alcohols onto hydroxylated surfaces such as $Zn(OH)_2$,[2] $Al(OH)_3$,[3] AlOOH,[4] and ZnAl LDHs.[5] These reports point out the specific reactivity of hydroxyl layers toward some organic molecules. On the other hand, using thermal treatments, we have grafted oxoanions onto LDH layers, showing the ability of the double hydroxide layers to incorporate anionic oxides into their layers. Consequently, LDHs containing sulfate, chromate, and dichromate[6,7] undergo a strong interlamellar contraction of nearly 0.2 nm due to the replacement of OH groups of the layers by oxygen atoms of the oxoanions. This behavior is not reversible and leads to a strong increase in the structure stability. Delmas et al.[8] have reported similar phenomena with vanadate and polyvanadate. In the same way, we have shown the polymerization and the grafting of silicate layers in LDH.[9]

For this study, layered double hydroxide materials (LDHs) described by the formula $[M^{II}_{1-x}M^{III}_x(OH)_2][A^{m-}_{x/m}\cdot nH_2O]$ are chosen as inorganic host structures for their high anion exchange capacities and their layer reactivities. Tartrate (^-O_2C-$(CHOH)_2CO_2^-$), with its two carboxylate groups and its two condensable OH groups, appears to be an appropriate guest molecule for the preparation of new stable hybrid LDHs. A comparative study with the succinate anion ($^-O_2C(CH_2)_2CO_2^-$), similar to tartrate without the OH functions, allows us to evaluate the effect of the OH groups in the host/guest interactions. Intercalation of tartrate and succinate anions in LDH and thermal treatments of the hybrid phases are presented here. This study concerns the four different LDH phases $[Zn_3Al(OH)_8](C_4H_4$-$O_6)_{0.5}\cdot nH_2O$, $[Zn_2Cr(OH)_6](C_4H_4O_6)_{0.5}\cdot nH_2O$, $[Zn_3Al(OH)_8]$-

* Corresponding author. E-mail: Forano@cicc.univ-bpclermont.fr.

(1) Sanchez C. *Matériaux hybrides*; Observatoire Français des Techniques Avancées, Masso: Paris, 1996; p 27.
(2) Tagaya, H.; Ogata, S.; Morioka, H.; Kadokawa, J.; Karasu, M.; Chiba, K. *J. Mater. Chem.* **1996**, *6*, 1235.
(3) Inoue, M.; Kominami, H.; Kondo, Y.; Inui, T. *Chem. Mater.* **1997**, *9*, 1614.
(4) Inoue, M.; Kondo, Y.; Inui, T. *Inorg. Chem.* **1988**, *27*, 215.
(5) Morioka, H.; Tagaya, H.; Karasu, M.; Chiba, K. *J. Solid State Chem.* **1995**, *117*, 337.
(6) Depege, C.; Forano, C.; de Roy, A.; Besse, J. P. *Mol. Cryst. Liq. Cryst.*, **1994**, *244*, 161.
(7) Forano, C.; de Roy, A.; Depege, C.; Khaldi, M.; El Metoui, F. Z.; Besse, J. P. In *Synthesis of Porous Materials: Zeolites, Clays and Nanostructures*; Occelli, M. L., Kessler, H., Eds.; Marcel Dekker: New York, 1996; p 607.
(8) Menetrier, M.; Khan, K. S.; Guerlou-Demourgues, L.; Delmas, C. *Inorg. Chem.* **1997**, *36*, 2441.
(9) Depege, C.; El Metoui, F. Z.; Forano, C.; de Roy, A.; Dupuis, J.; Besse, J. P. *Chem. Mater.* **1996**, *8*, 952.

S0020-1669(98)00123-2 CCC: $15.00
Published on Web 08/07/1998

Table 1. Chemical Compositions of Precursor Compounds and the Tartrate and Succinate Derivatives

LDH abbreviated formula	M^{2+}/M^{3+}	anion/Al^{3+}	H_2O/Al^{3+}
$[Zn_3AlCl]$	3.1	1.2	2.0
$[Zn_3AlCO_3]$	3.0	0.6	2.4
$[Zn_3AlTar]$	2.9	0.7	2.6
$[Zn_3AlSuc]$	2.7	0.7	2.5
$[Zn_2CrCl]$	2.0	1.0	1.9
$[Zn_2CrTar]$	1.7	0.6	2.2
$[Zn_2CrSuc]$	1.7	0.6	3.0

$(C_4H_6O_4)_{0.5}\cdot nH_2O$, and $[Zn_2Cr(OH)_6](C_4H_6O_4)_{0.5}\cdot nH_2O$, noted more simply as Zn_3AlTar, Zn_2CrTar, Zn_3AlSuc, and Zn_2CrSuc. The thermal stabilities of the various phases are presented.

Experimental Section

Synthesis. The materials were prepared via three different methods: anion exchange on LDH precursor, direct coprecipitation,[10] and reconstruction of the LDH phase from calcined LDH derivatives. A recent review of the various syntheses of organic anions containing LDHs was published by Carlino.[11]

Coprecipitation. (a) Preparation of Zn_3AlCl. Zn_3AlCl was prepared by coprecipitation as follows: A 40 mL portion of a zinc chloride (0.75 M) and aluminum chloride (0.25 M) solution was added at a rate of 0.16 mL·min^{-1} in a flask containing 150 mL of distilled and deionized water, at room temperature, under a nitrogen atmosphere (in order to minimize the contamination with atmospheric CO_2) and under vigorous stirring. A solution of sodium hydroxide (1 M) was simultaneously added. This addition was realized using an automated titrator monitored by a pH regulator via a pH electrode immersed in the reagent solution in order to fix the pH of coprecipitation at 8.0 ± 0.2. The addition of the metallic salt solution was completed in 4 h, and the mixture was then left to react for 36 h. The LDH was recovered by three dispersion and centrifugation cycles in deionized water, with a 1% mass ratio of solid in suspension. The obtained gelatinous precipitate was finally air-dried. The chemical analysis (Table 1) confirms a typical composition of anionic clays with a Zn^{2+}/Al^{3+} ratio of 3.00. A hydration state of 2.5 H_2O molecules per Al^{3+} cation was measured by TGA.

(b) Preparation of Zn_2CrCl. Zn_2CrCl was prepared by coprecipitation similarly to Zn_3AlCl with 40 mL of zinc chloride (0.66 M) and chromium chloride (0.33 M) solution. The pH of coprecipitation was fixed at 5.5 ± 0.2. The chemical analysis is given in Table 1.

(c) Preparation of Zn_3AlCO_3. Zn_3AlCO_3 was coprecipitated, according to a previously published procedure,[12] at pH = 9.0, from a 1 M metallic nitrate solution of Zn^{2+} and Al^{3+} with a Zn^{2+}/Al^{3+} molar ratio of 3.0 and a mixed solution of sodium hydroxide (0.40 M) and sodium carbonate (0.12 M).

(d) Preparation of Zn_3AlTar and Zn_3AlSuc. Conditions similar to those for the coprecipitation of Zn_3AlCl were used. Sodium tartrate or sodium succinate was initially introduced into the reactor with a (Tar or Suc)/Al^{3+} molar ratio of 10.0. The synthesis was performed at room temperature.

Anion Exchange. (a) Preparation of Zn_3AlTar and Zn_2CrTar. Tartrate exchanges were performed on the chloride LDH precursors at fixed pH values of 8.0 and 5.5, respectively. An excess of 10 equiv of tartrate anions over the Al^{3+} or Cr^{3+} content was used. All the preparative procedures were performed with deionized water, under stirring and a nitrogen atmosphere. The precipitates were recovered from their mother liquors by repeated centrifugation−washing cycles.

(b) Preparation of Zn_3AlSuc and Zn_2CrSuc. Exchanges were realized identically to those for Zn_3AlTar and Zn_2CrTar.

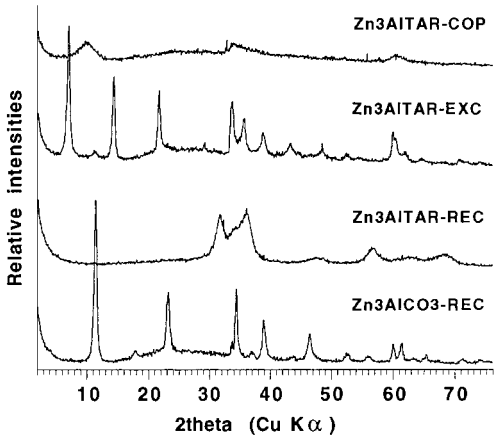

Figure 1. PXRD patterns of ZnAlTar prepared by coprecipitation (COP), exchange (EXC), and reconstruction (REC) and $ZnAlCO_3$ prepared by reconstruction.

Reconstruction: Preparation of Zn_3AlTar. The reconstruction method was carried out on the Zn_3AlCO_3 phase calcined at 200, 300, and 400 °C. The Zn−Al mixed oxides were suspended in an aqueous solution containing the tartrate sodium salt under a nitrogen atmosphere to prevent any reconstruction of a carbonate LDH phase. The Tar^{2-}/Al^{3+} ratio was fixed at 10.0.

Physical Measurements. Powder X-ray diffraction (PXRD) patterns were obtained with a Siemens D501 X-ray diffractometer using Cu Kα radiation and fitted with a graphite back-end monochromator. Fourier transform infrared (FTIR) spectra were recorded on a Perkin-Elmer 16PC spectrophotometer on pressed KBr pellets. Thermogravimetric analyses (TGA) were performed with a Setaram TG-DTA92 thermogravimetric analyzer at a typical rate of 5 °C/min under an air atmosphere. Chemical analyses (Zn, Al, Cr, Cl, H, C) were performed in the Vernaison Analysis Center of the CNRS. High-resolution solid-state NMR spectra were obtained with a Bruker MSL-300 spectrometer. ^{13}C CP-MAS NMR spectra were recorded with a $\pi/2$ impulsion delay of 10 μs, an acquisition time of 2 s, and a contact time of 20 ms. ^1H decoupling was applied during FID recording. The chemical shifts are given in ppm relative to TMS as the external reference. The N_2 adsorption isotherms of the samples were recorded on a Fison SP1920 instrument. Prior to the sorption experiments, the materials were subjected to a pretreatment which consisted of heating in air at 150 °C for one night to remove adsorbed water.

Results and Discussion

Preparation Methods and Chemical Analyses. The preparation of Zn_3AlTar was performed by three different methods: the coprecipitation at a fixed pH of the double metallic hydroxides in an aqueous solution containing the organic salt, the anion exchange reaction on the chloride LDH precursor, and the calcination−reconstruction method. PXRD patterns of some samples of Zn_3AlTar prepared by these methods are given in Figure 1.

Only the anion exchange yielded pure and well-crystallized Zn_3AlTar. The low intense diffraction line at 11.4° (2θ) corresponds to a small contamination by a carbonate LDH phase; such a contamination is often unavoidable during anion exchange and occurs during the washing steps performed under air. Meyn and co-workers have already reported[13] the anion exchange of Zn_3Al and Zn_2Cr with tartrate and succinate. They mentioned that tartrate does not exchange as easily as the other alkanedioic acids; the degree of exchange is low and the 00*l* reflections are broader.They used Tar^{2-}/Al^{3+} ratios lower than 2.0. We observed that the use of a Tar^{2-}/Al^{3+} ratio of 10.0 is needed to improve both purity and crystallinity. Exchange in

(10) Park, I. Y.; Kuroda, K.; Kato, C. *J. Chem. Soc., Dalton Trans.* **1990**, 3071.
(11) Carlino, S. *Solid State Ionics* **1997**, *98*, 73.
(12) Thévenot, F.; Szymansky, R.; Chaumette, P. *Clays Clay Miner.* **1989**, *37*, 396.
(13) Meyn, M.; Beneke, K.; Lagaly, G. *Inorg. Chem.* **1990**, *29*, 5201.

an autoclave at various temperatures from 40 °C up to 120 °C during 4 days did not improve the crystallinity of the products.

The coprecipitation method was realized at different pHs, from 8.0 to 10.0, and different Tar^{2-}/Al^{3+} ratios, from 2.0 to 10.0, at room temperature or under reflux conditions. Usually, compounds of high purity and crystallinity are obtained by this method,[14] particularly LDH materials with organic ions.[15] However, in the presence of tartrate, we obtained LDH phases of very poor crystallinity. The presence of more or less important quantities of an amorphous component was often observed.

The reconstruction method was reported in the literature[16] as an alternative pathway for the preparation of hybrid LDHs. Zn_3AlCO_3 was calcined at 200, 300, and 400 °C. The calcined phases were rehydrated in aqueous solutions containing tartrate anions with an excess of 10.0 mol/mol of Al^{3+}. No reconstruction of the LDH phase was observed, and ZnO was present in all phases. Using the same conditions in the presence of Na_2CO_3, we obtained Zn_3AlCO_3. The cause of the restricted reaction is the complexing power of the tartrate anions, which react spontaneously with metallic cations and oxides, impeding LDH synthesis.

Like Zn_3AlTar, pure Zn_2CrTar could only be prepared by an anion exchange reaction at room temperature or under hydrothermal conditions in an autoclave at 120 °C. Intercalation of tartrate was confirmed by XRD and IR spectroscopy. For succinate anions, coprecipitation and anion exchange were successful as the consequence of the lower reactivity of succinate toward metal cations.

The chemical compositions for the LDH phases of highest purity obtained by elemental analyses are given in Table 1. The water content was determined by TG. The experimental M^{II}/M^{III} ratio was near the initial value of the starting salt solutions, when the coprecipitation pH value was carefully chosen. The excess of carbon (the expected anion/Al^{3+} ratio would be equal to 0.5) results from adsorption of the anions on the LDH surface.

Powder X-ray Diffraction. The PXRD patterns of all the phases are typical of layered materials of relatively good crystallinity (Figure 2). However, for the organic derivative compounds, as is often the case,[15] several of the (*hkl*) reflections disappeared or were broadened. This is typical of a turbostratic effect caused by a decrease of the ordering along the stacking axis due to the loss of the van der Waals interaction between adjacents layer and the absence of a densely packed interlayer space formed by high-charge-density anions such as halides or oxoanions.

The reflections of all the phases were indexed in a hexagonal lattice with an $R\bar{3}m$ rhombohedral symmetry (Table 2). Attempts have been made to refine the PXR diffractions of the various LDH phases in the hexagonal lattice with a primitive mode 1H or 2H, but some mismatchings between observed and calculated reflections lead us to reject these systems.

The intercalation of the organic molecules inside the lamellar host structure is clearly evidenced in all the cases by the net increase of the basal spacing d_{bs} from 0.781 and 0.786 nm for the precursors Zn_2CrCl and Zn_3AlCl, respectively, to 1.155−1.224 nm for the organic derivatives. Similar values were obtained by Meyn et al.[13] for succinate- and tartrate-containing

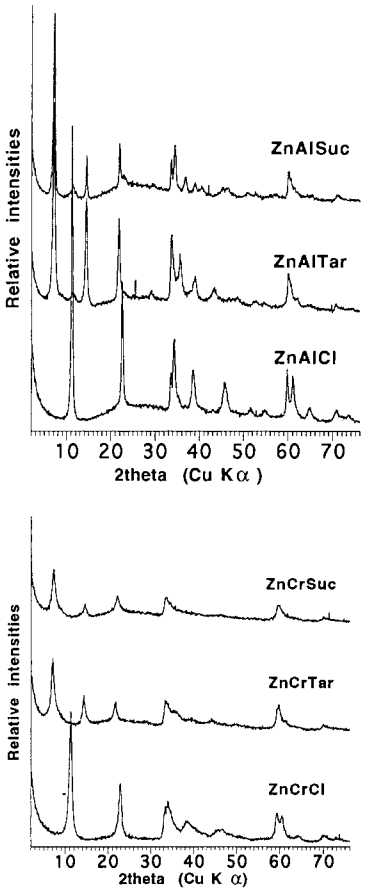

Figure 2. PXRD patterns of chloride precursor LDHs and organic derivatives.

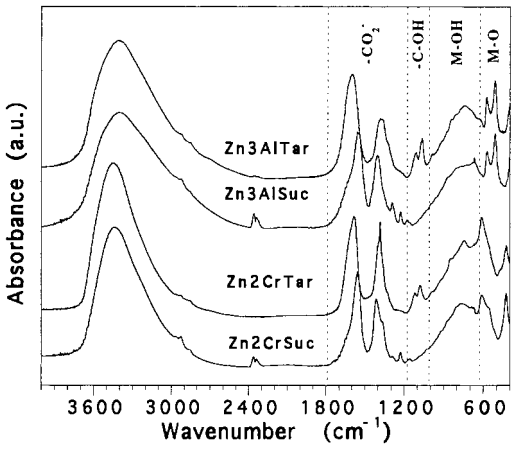

Figure 3. FTIR spectra of Zn_2CrSuc, Zn_2CrTar, Zn_3AlSuc, and Zn_3AlTar.

LDHs, prepared by anion exchange reactions on Zn_2AlNO_3 and Zn_2CrNO_3. The basal spacing is obviously not affected by a change in the charge density of the layers, from 0.041 e/Å^2 for Zn_2Cr to 0.030 e/Å^2 for Zn_3Al. Thus, the interlayer distance is mainly determined by the orientation of the organic anions in the interlamellar space.

Infrared Spectroscopy. The intercalation is also confirmed by FTIR spectroscopy (Figure 3). All stretching and bending vibration modes of the organic anions are observed, besides the absorption bands of the hydroxylated layers. The vibration bands were assigned in comparison with the Raman and IR spectra of the dipotassium tartrate hemihydrate (Bhattacharjee et al.).[17]

(14) de Roy, A.; Forano, C.; El Malki, K.; Besse, J. P. *Anionic Clays: Trends in Pillaring Chemistry. Synthesis of Microporous Materials*; Occelli, L., Robson, H., Eds.; Van Nostrand Reinhold: New York, 1992; Vol. 2, p 108.
(15) Bonnet, S.; Forano, C.; de Roy, A.; Besse, J. P.; Maillard, P.; Momenteau, M. *Chem. Mater.* **1996**, *8*, 1962.
(16) Sato, T.; Okuwaki, A. *Solid State Ionics* **1991**, *45*, 43.

Table 2. d_{hkl} Distances and Refined Unit Cell Parameters for the Chloride Precursor LDHs and Organic Derivatives

	Zn_3AlCl		Zn_3AlTar		Zn_3AlSuc		Zn_2CrCl		Zn_2CrTar		Zn_2CrSuc	
hkl	d_{obs} (Å)	d_{calc} (Å)	d_{obs} (Å)	d_{calc} (Å)	d_{obs} (Å)	d_{calc} (Å)	d_{obs} (Å)	d_{calc} (Å)	d_{obs} (Å)	d_{calc} (Å)	d_{obs} (Å)	d_{calc} (Å)
003	7.861	7.860	12.308	12.236	12.341	12.140	7.803	7.806	12.340	12.241	12.181	12.181
006	3.931	3.930	6.123	6.118	6.099	6.070	3.882	3.903	6.136	6.121	6.055	6.091
009			4.070	4.078	4.035	4.047			4.083	4.080	4.013	4.060
0,0,12			3.057	3.059	3.036	3.035						
101	2.662	2.655	2.659	2.660	2.665	2.658	2.681	2.680	2.685	2.677	2.681	2.681
012	2.603	2.606	2.642	2.639			2.627	2.629			2.661	2.660
104	2.438	2.434	2.558	2.561							2.604	2.579
015	2.327	2.325	2.514	2.507			2.337	2.338	2.522	2.521	2.524	2.523
107	2.097	2.094					2.113	2.100				
018	1.981	1.980	2.308	2.306			1.985	1.984				
10,1,0	1.769	1.768										
0,1,11	1.671	1.672	2.083	2.083					2.040	2.040		
0,1,14			1.871	1.870								
1,0,16			1.734	1.739								
0,1,17			1.677	1.678								
110	1.544	1.543	1.539	1.540	1.539	1.539	1.556	1.558	1.549	1.550	1.551	1.552
0,0,24			1.531	1.530	1.528	1.527					1.523	1.523
113	1.515	1.514					1.529	1.528			1.540	1.540
116	1.437	1.436	1.494	1.493			1.449	1.447				
021	1.332	1.334	1.333	1.332	1.331	1.332	1.345	1.347			1.343	1.343
a (nm)	0.3086		0.3079		0.3078		0.31157		0.3099		0.3104	
c (nm)	2.358		3.671		3.464		2.342		3.672		3.654	
r^a	0.0012		0.0013		0.0016		0.0021		0.0014		0.0031	
d_{bs} (nm)	0.786		1.224		1.155		0.781		1.224		1.218	
$d_{bs}{}^b$ (nm)			1.22		1.20				1.21		1.22	

^{a} $r = \{[\sum_i(1/d_{i(obs)} - 1/d_{i(calc)})^2]/[\sum_i 1/d_{i(obs)}{}^2]\}^2$. ^{b} Data from ref 2.

Table 3. Carboxylate IR Vibrations (cm^{-1}) of the LDHs Intercalated with Tartrate and Succinate

	NaTar	NaSuc	Zn_3-AlTar	Zn_2-CrTar	Zn_3-AlSuc	Zn_2-CrSuc
$\nu_{as}(-CO_2)$	1626	1576	1587	1587	1560	1548
$\nu_s(-CO_2)$	1422	1447	1400	1390	1412	1403
$\Delta\nu = \nu_{as} - \nu_s$	204	129	187	197	148	145

The ν_s and ν_{as} stretching vibrations of $-CO_2^-$ of the intercalated tartrate and succinate anions are given in Table 3 and compared with the corresponding values of the sodium salts. According to Nakamoto,[18] the difference $\Delta\nu = \nu_{as} - \nu_s$ gives information about the symmetry of the interaction between the carboxylate $-CO_2^-$ group and the hydroxylated layers. With $\Delta\nu$ values nearly similar to those of the sodium salts, bridging by both oxygen ions of the carboxylate to the layer hydroxyls seems to be probable.

After intercalation, the five OH valence stretching bands of the two alcohol groups, in the range 3206−3565 cm^{-1} for the sodium salt, are reduced in one band, centered under the OH vibration of the layer hydroxyls, at 3456 cm^{-1} for Zn_3AlTar and 3402 cm^{-1} for Zn_2CrTar. This evidences strong hydrogen bonding between C−O−H and layer hydroxyls or internal water molecules.

The intercalation of the tartrate anion does not affect the two ν_{COH} stretching vibrations of the alcoholic groups, which remain at the same wavenumbers, 1128 and 1078 cm^{-1} for NaTar, 1121 and 1080 cm^{-1} for Zn_3AlTar, and 1121 and 1081 cm^{-1} for Zn_2-CrTar.

Structural Evolution under Moderate Thermal Treatment. To study the reactivity of tartrate and succinate anions with the host structure, the samples were treated to 150 °C (calcined phases are noted $M^{II}M^{III}X$-Cal). The thermal treatment of all organic derivatives contracted the interlamellar distance (Figure 4). Calcination did not strongly affect the crystallinity of the phases.

Table 4. Basal Spacings (*d*) and Refined Unit Cell Parameters for the Prepared LDHs and Calcined Derivatives

LDH	*a* (nm)	*c* (nm)	*d* (nm)	Δ*d* (nm)
Zn_3AlTar	0.3079(4)	3.671(5)	1.224(1)	0.253
Zn_3AlTar-Cal	0.3078(6)	2.912(6)	0.971(2)	
Zn_2CrTar	0.3099(4)	3.672(5)	1.244(2)	0.272
Zn_2CrTar-Cal	0.3091(5)	2.856(5)	0.952(2)	
Zn_3AlSuc	0.3078(5)	3.464(5)	1.155(2)	0.233
Zn_3AlSuc-Cal	0.3086(5)	0.922(2)	0.922(2)	
Zn_2CrSuc	0.3104(9)	3.65(1)	1.218(4)	0.320
Zn_2CrSuc-Cal	0.3100(6)	2.695(6)	0.898(2)	

The contraction is 0.25 ± 0.02 and 0.32 nm for ZnCrSuc (Table 4). The unit cell parameters were refined with a 3R stacking sequence for all phases except for ZnAlSuc-Cal which clearly displayed a 1H mode.

Contraction of Zn_3AlTar occurred in a very small temperature range (Figure 5), between 70 and 90 °C, the basal spacing remaining nearly constant before and after the transition. This phenomenon is different from the contraction of LDHs containing oxoanions such as SO_4^{2-}, CrO_4^{2-}, and $Cr_2O_4^{2-}$,[6,9] which occurs continuously from room temperature up to 120 °C simultaneously with a departure of water.

Similar contractions are observed for LDH Zn_3AlSuc, Zn_2-CrTar, and Zn_2CrSuc. The higher concentration of interlayer species in Zn_2Cr LDH (33% higher than for Zn_3Al LDH) did not prevent the internal rearrangement.

We present in Figure 6 FTIR spectra of calcined Zn_3AlTar showing the ν_s and ν_{as} COO^- stretching bands and the δ_{COH} bending mode. All the bands remain nearly unaffected by the calcination. Only a slight broadening of the bands is observed with a small shift of the ν_{as} COO^- stretching to higher

(17) Bhattacharjee, R.; Jain, Y. S.; Bist, H. D. *J. Raman Spectrosc.* **1989**, *20*, 561.
(18) Nakamoto, K. *Infrared and Raman Spectra of Inorganic and Coordination Compounds*; John Wiley & Sons: New York, 1986.

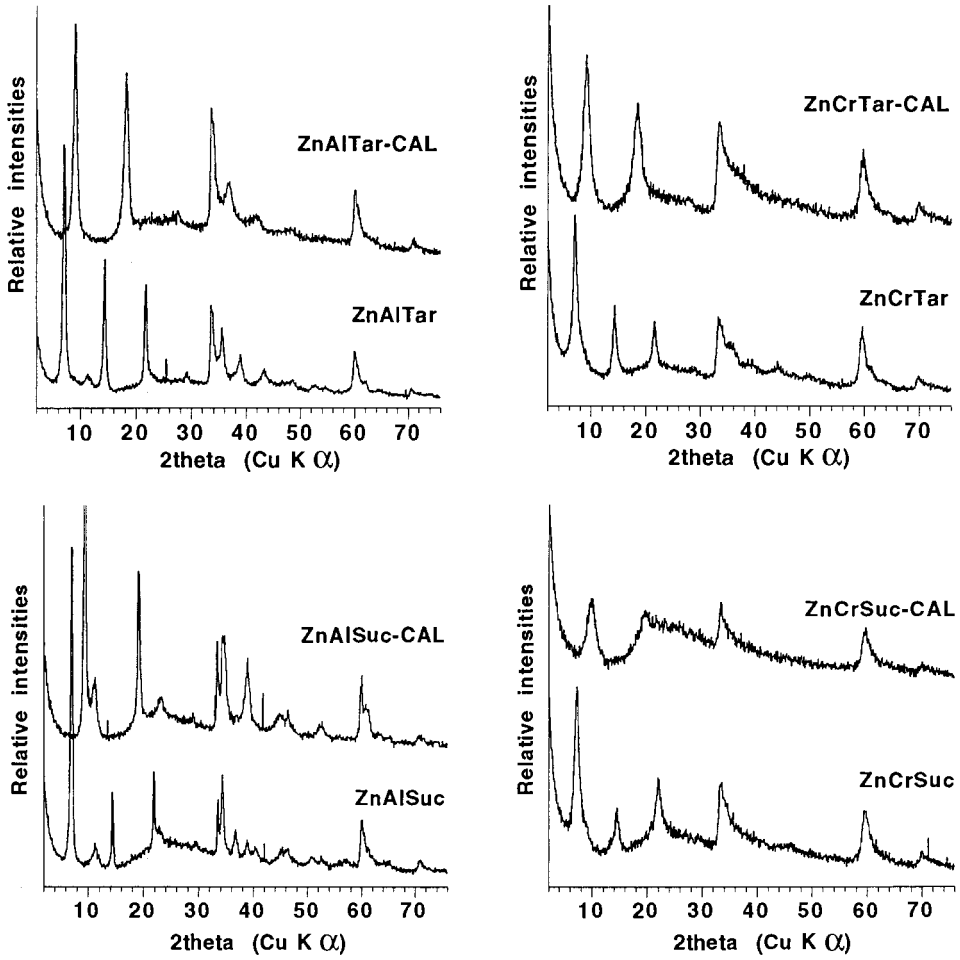

Figure 4. PXRD patterns of the LDHs intercalated with tartrate and succinate and the derivatives calcined at 150 °C.

frequencies corresponding to a slight lowering of the interaction with the layer due to the new stereochemical configuration of the carboxylate groups in the calcined phases. The organic molecules are not grafted onto the layer. Under calcination, the LDH phase reacts with CO_2 from air, resulting in adsorption of carbonate, as indicated by the increase of the typical thin and intense ν_3 stretching band of the CO_3^{2-} anion at 1385 cm^{-1}.

The analogies between calcined tartrate and succinate LDHs confirm that the alcoholic groups of the tartrate anions do not undergo any condensation during the contraction. The anions undergo only a stereochemical rearrangement without any bond breaking. This result is also confirmed by ^{13}C CPMAS NMR spectroscopy (Figure 7); the chemical shifts for the carboxylate and the hydroxy carbons remain unchanged before and after calcination, respectively at 183 and 75 ppm. Thus, the structure of the guest molecules is not affected by the contraction process.

In the DTG curves of Zn_3AlTar and Zn_3AlSuc untreated and 150 °C calcined phases (Figure 8), the first dehydration peak disappeared after calcination. The dehydration is not reversible; no rehydration of the calcined phases back to the hydrated precursors was obtained either at room temperature or in a 393 K heated autoclave during 2 weeks. These tests confirm that the contraction strengthens the interactions between the guest molecules and the host structure. In the case of Tar-containing LDH, the new orientation of the anion allows the creation of hydrogen bonds between OH groups of both partners. Indeed, in a perpendicular orientation $^{-}O_2C-CHOH-CHOH-CO_2^{-}$ orientates its two $-CO_2^{-}$ groups toward the $[M^{II}_{1-x}M^{III}_{x}(OH)_2]$ planes. Tartrate then acts as a bridge attached to both adjacent layers via one hydrogen bond. When tartrate is in a flat position, additive H-bonding occurs from alcohol groups. This leads to an increase of the thermal and chemical stability (see below). However the compound was not rehydrated under dynamic vacuum at room temperature.

Structural Model of the Contraction. All the experimental results indicate that the tartrate and succinate anions are intercalated in the interlayer space and bound by electrostatic interactions and hydrogen bonds to the host matrix. If the layer thickness (0.21 nm) and the hydrogen-bond distances between guest and host (0.27 ± 0.01 nm) are subtracted from the basal spacing,[19] the distance of the interlayer space (d_{is}) (Figure 9a), available for the anions, can be calculated. Values of d_{is} are 0.474 and 0.221 nm, respectively, for Zn_3AlTar and Zn_3AlTar-Cal. Comparison with the size of the tartrate anion in an anti conformation (0.477 nm) indicates a perpendicular and a flat orientation of the tartrate. Thus, the structural changes at 80 °C corresponds to the reorientation of the organic anion, probably around the central C_2-C_3 bond. This reorientation occurs simultaneously with the desorption of interlayer water molecules as confirmed by the DTG curves. We show the idealized structures in Figure 9b. Similar rearrangements and structures are assumed to occur in the presence of the succinate anion.

The increase of stability after the contraction was confirmed by unsuccessful attempts to exchange the tartrate ions with carbonate ions despite the fact that the layered hydroxides display a very high affinity for CO_3^{2-}. In contrast, the

(19) Therias, S.; Mousty, C.; Bonnet, S.; Forano, C.; Palvadeau, P. *Mol. Cryst. Liq. Cryst.*, in press.

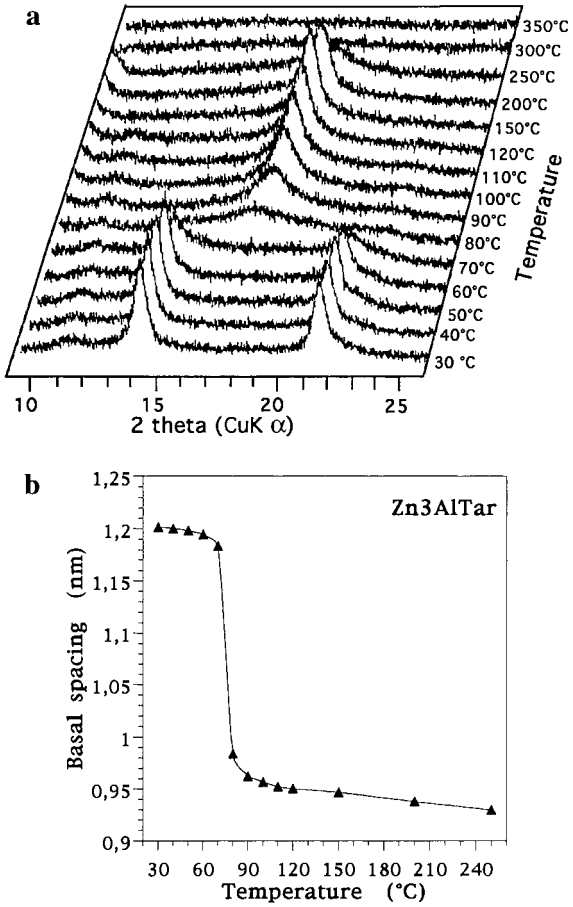

Figure 5. PXRD patterns (a) and basal spacing (b) versus temperature for Zn_3AlTar.

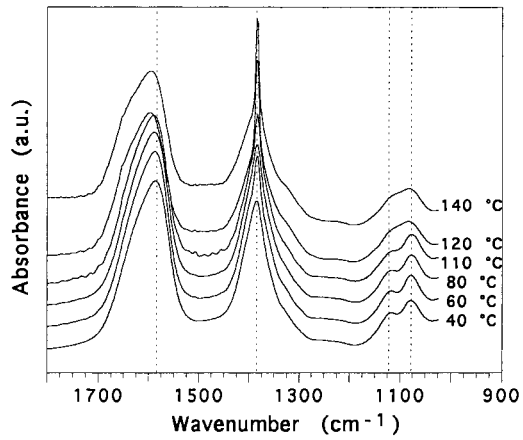

Figure 6. FTIR spectra of Zn_3AlTar calcined at different temperatures.

as-prepared Zn_3AlTar exchanges all tartrate ions with CO_3^{2-}, leading to an interlamellar distance of 0.76 nm. For the calcined phase, Zn_3AlTar-Cal, only a partial exchange was observed. The XRD pattern showed the coexistence of both Zn_3AlCO_3 and Zn_3AlTar. In contrast, exchange of Zn_3AlSuc and Zn_3AlSuc-Cal with CO_3^{2-} resulted in the pure Zn_3AlCO_3 phase.

Thermal and Structural Stability

TGA and DTA. As shown by the DTA curves (Figure 10), two very different decomposition domains are involved. The endothermic events observed up to 250 or 300 °C for Zn_2Cr and Zn_3Al are due to the desorption of adsorbed and intercalated water and then to the dehydroxylation of the layer. The different

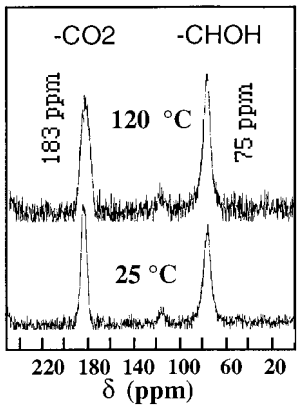

Figure 7. CPMAS ^{13}C NMR of untreated and calcined [Zn_3AlTar] LDH.

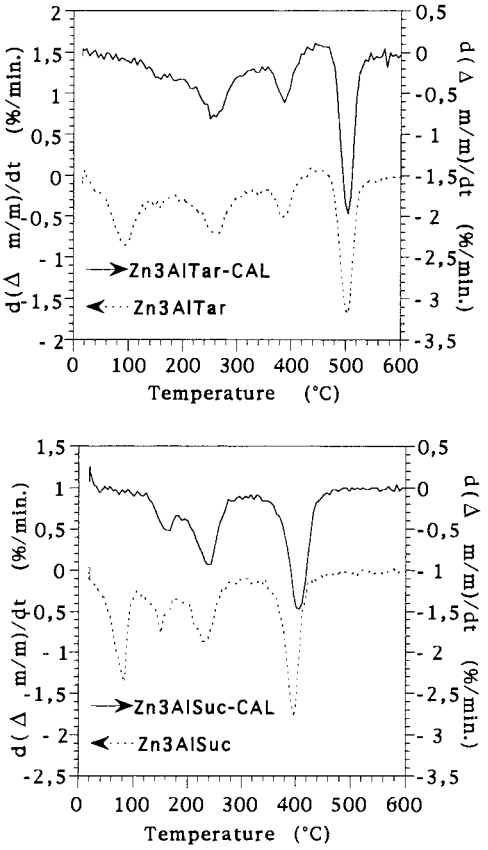

Figure 8. DTG curves of Zn_3AlTar, Zn_3AlTar-Cal, Zn_3AlSuc, and Zn_3AlSuc-Cal.

reactions are clearly identified by the DTG curves in Figure 8. TGA (under air, at relative humidity pressure higher than 70% or under argon) indicates the same dehydration processes. No clear effect of the ambient humidity is observed. The stability of the hydrated compounds mainly results from the energy of interaction between the water molecules and the layered host structure and from the bonding energy within the metal hydroxide layers. Above these temperatures, a strong exothermic signal indicates the organic anions decompose in one step only for Zn_3AlTar. At least three thermal events are involved; one intermediate corresponds to a weight gain due to an oxidation process. Complementary analyses are presently performed by coupling a mass analyzer to the TGA/DTA apparatus in order to elucidate the mechanism of decomposition of the organic entities. These measurements clearly evidence a specific reactivity of tartrate with the ZnAl LDH layers.

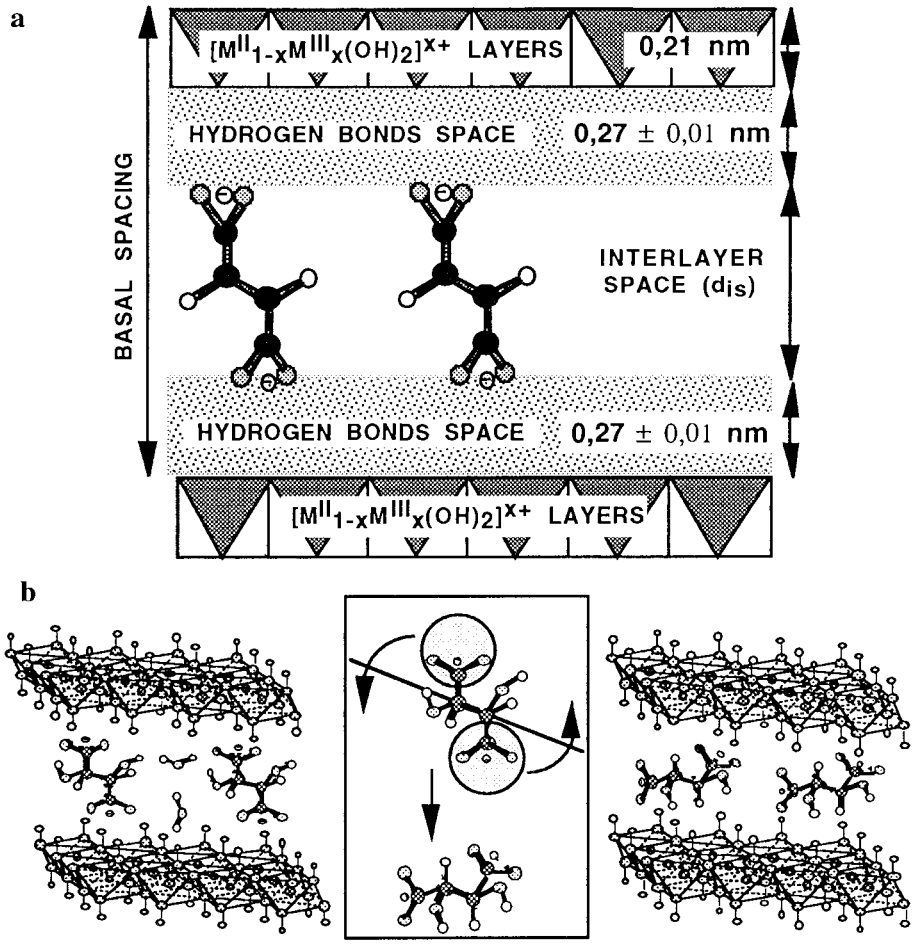

Figure 9. Model for the reorientation of the tartrate anion between the hydroxylated layers.

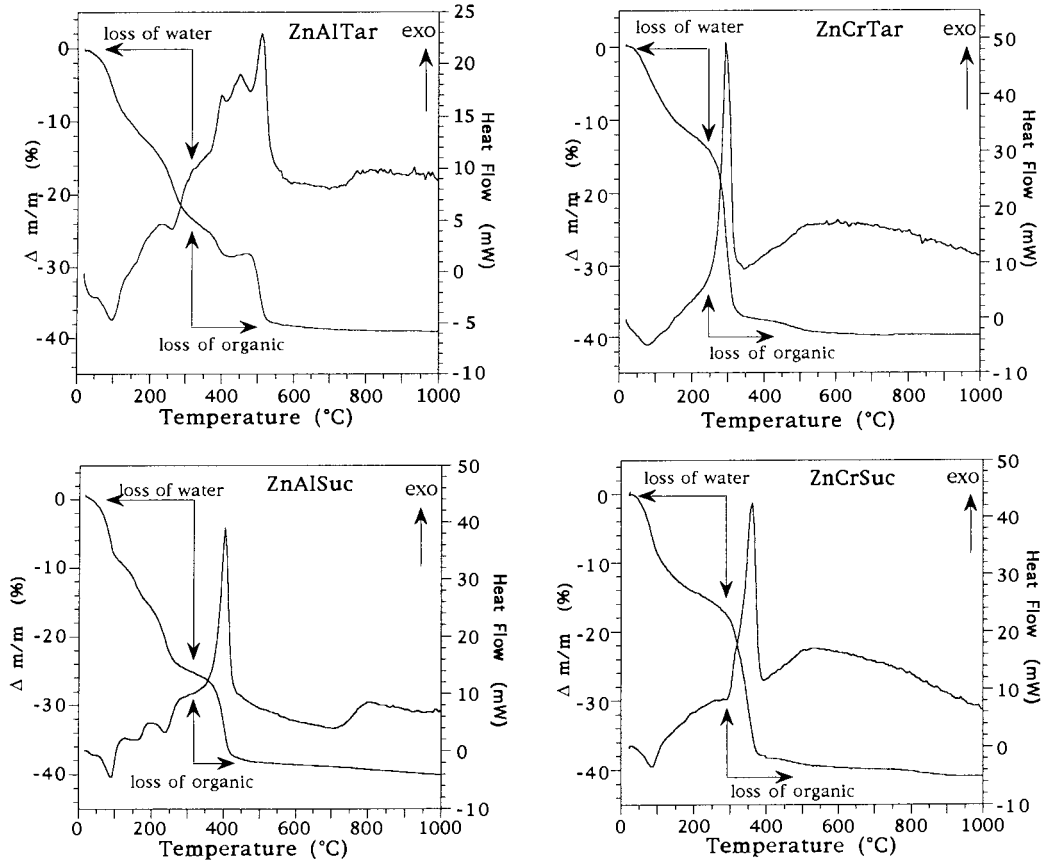

Figure 10. TGA and DTA of Zn_3AlTar, Zn_2CrTar, Zn_3AlSuc, and Zn_2CrSuc.

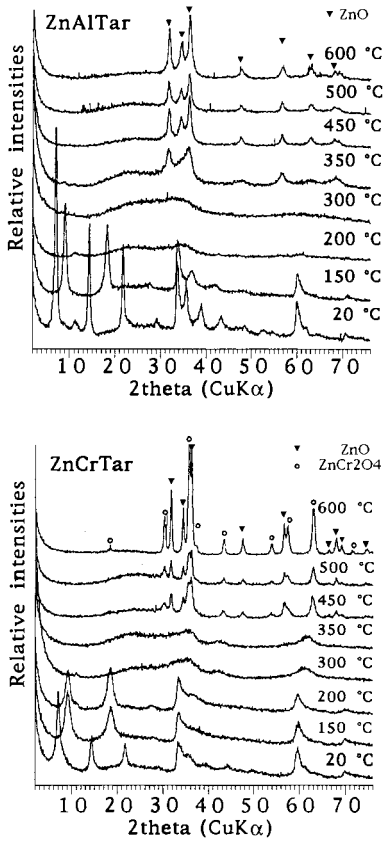

Figure 11. PXRD patterns of Zn_3AlTar and Zn_2CrTar phases calcined at various temperatures.

Unexpectedly, the quantitative analyses of the ZnAlTar thermogram cannot account for the total removal of the organic entity. The gray color of the residual calcined compound confirms the presence of carbon in the final product.

As usually shown,[20] the Zn_2Cr matrix is less stable than the Zn_3Al matrix and begins to dehydroxylate at a temperature 80 °C lower than ZnAl LDH.

XRD. The structure of Zn_3AlTar (Figure 11) collapses at a temperature above 150 °C. The thermal decomposition led to a metastable amorphous oxide mixture which transformed in ZnO and in the spinel phase $ZnAl_2O_4$. ZnO appeared at 350 °C, but the spinel phase did not crystallize below 600 °C. We note a delay of 100 °C in the formation of ZnO compared to calcination of Zn_3AlCl although the decomposition of the anions occurred in the same range of temperature.

The presence of tartrate ions increases the thermal stability of Zn_2Cr, which dexhydroxylates at a temperature 50 °C higher than usually observed for the chloride precursor. The crystallization of ZnO and the spinel $ZnCr_2O_4$ occurred simultaneously at 450 °C, 100 °C higher than for the calcination of Zn_2CrCl. Thus, the tartrate has the same stabilizing effect on the host matrix than oxoanions such as CrO_4^- or SO_4^{2-}.

We conclude that the decomposition of tartrate and succinate LDHs is similar to that of the parent LDH and differs from that of LDHs with aromatic anionic molecules such as terephthalate,[14] *meso*-tetrakis(*p*-carboxyphenyl)porphyrin (pTCPP), or meso-tetrakis(*p*-sulfonatophenyl)porphyrin (pTSPP).[21] The mineral host structure of these organic materials decomposed before the decomposition of the organic ions. This led to new organic oxides, obtained at 350 °C, which retain a layered structure and delayed, under thermal decomposition, the crystallization of the metallic oxides at higher temperatures.

Table 5. BET Specific Surface Areas for Calcined ZnAlTar and ZnCrTar

	T (°C)					
	150	200	350	450	500	600
Zn_3AlTar	24	22	77	93	58	63
Zn_2CrTar	69	53	79	29	32	
Zn_3AlCl[25]	29	71	36	35	38	20

Specific Surface Area. Synthetic LDH compounds are widely used as precursors for the preparation of mixed oxide catalysts.[22] We measured the porosity properties of the prepared compounds by BET nitrogen adsorption and desorption isotherms.[23] These macroscopic properties can be directly related to the inner structure of the bulk material and to its morphology.

The N_2 adsorption/desorption curves of the calcined Zn_3AlTar and Zn_2CrTar (Figure 12) are typical of mesoporous materials of type IV, according to the classification of BDDT.[24] A similar behavior was described for LDH reference materials such as ZnAl and ZnCr containing chloride or carbonate.[23] Intercalation in LDH of organic anions was considered as a possibility to prepare novel microporous or mesoporous pillared compounds or to modify the thermal decomposition process of the host structure in order to enhance the specific surface area and to influence the porosity of the derived mixed oxides. We recently reported[15] that intercalation of pTCPP and pTSPP in ZnAl LDH largely increased the BET specific surface area from 30 $m^2\ g^{-1}$ for the parent chloride material to 260 $m^2\ g^{-1}$ for the organic derivatives. The large organic ions are intercalated perpendicularly to the layers and create microporosity. The specific surface area of the tartrate LDHs calcined at 150 °C is low, 24 and 69 $m^2\ g^{-1}$, for Zn_3AlTar and Zn_2CrTar (Table 5). The value for Zn_3AlTar is similar to that of the chloride precursor. The distribution of pore volumes is large and is spread over the entire mesopore range; microporosity is not observed. This is due to the compact arrangement of the anions, lying flat and parallel to the layers. Strong and numerous hydrogen bonds between guest and host result in a very short basal spacing of 0.97 nm, much more shorter than 2.29 or 2.27 nm, respectively, for Zn_3-AlTSPP or $Zn_3AlTCPP$.

The specific surface area of the calcined phases never exceeded 100 $m^2\ g^{-1}$ as for the chloride precursors. They display quite similar thermal decomposition processes with rapid dehydration followed by a rapid crystallization of the metal oxides. This probably explains the low-surface-area properties of all these LDH phases.

Conclusions

During this study, we have stressed the different methods of synthesis of Zn_3Al and Zn_2Cr LDHs intercalated with either tartrate or succinate anions. Anion exchange appears to be a successful method for the intercalation of alkanedioate salts in LDH. If coprecipitation favors a high crystallinity, it is not suitable for an anion with reactive groups such as alcohol. As

(20) de Roy, A.; Vernay, A. M.; Besse, J. P.; Thomas, G. *Analysis* **1988**, *16*, 409.
(21) Bonnet, S. Synthèse et carcatérisation de matériaux hybrides de type HDL-Porphyrine. Thèse de Chimie, Université B. Pascal, Clermont-Ferrand, France; No. 27-03-1997.
(22) Vaccari, A., Ed. *Synthesis and Applications of Anionic Clays*; Elsevier: Amsterdam, 1995.
(23) Malherbe, F.; Forano, C.; Besse, J. P. *Microporous Mater.* **1997**, *10*, 67.
(24) Gregg, S. G.; Sing, K. S. W. *Adsorption, Surface Area and Porosity*; Academic Press: New York, 1982.
(25) Guyot, C. Laboratoire Matériaux Inorganiques, CNRS, Aubière, France. Private communication, 1993.

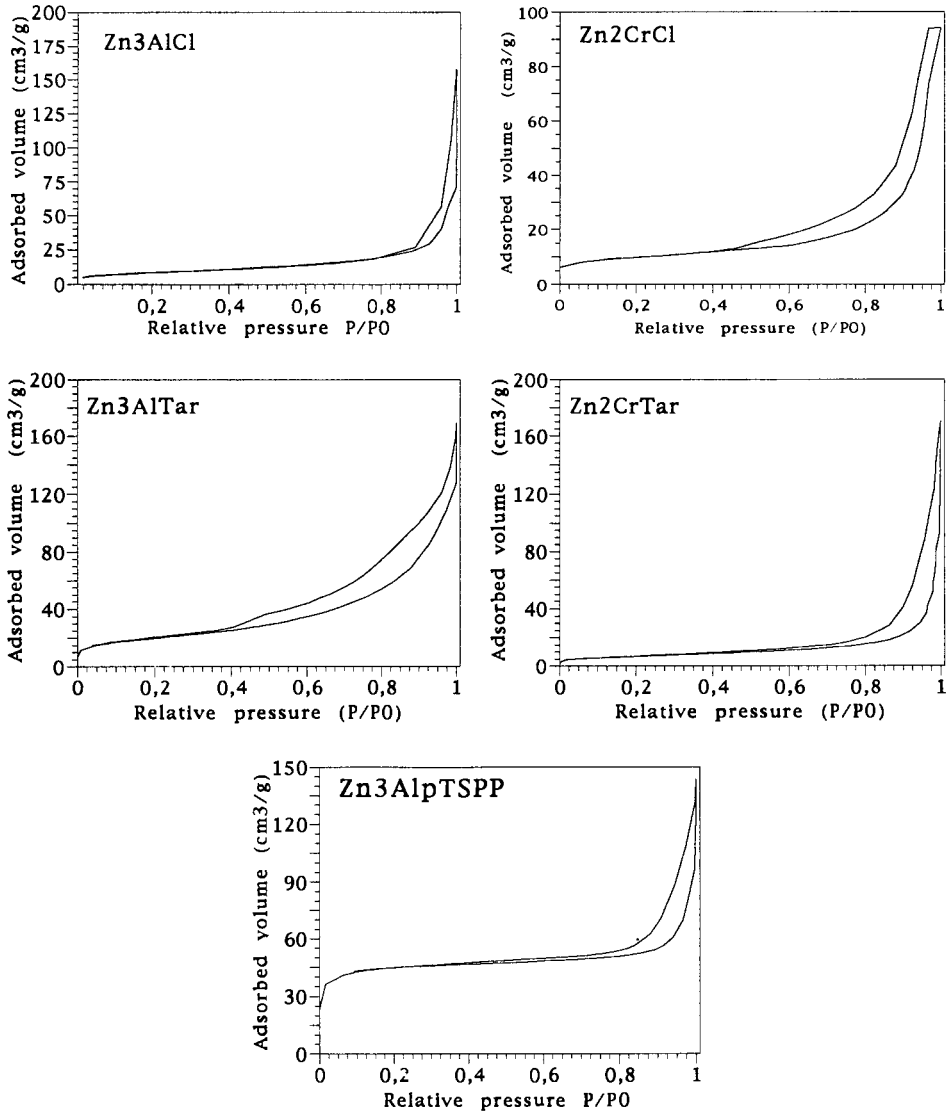

Figure 12. N_2 adsorption/desorption isotherms of Zn_3AlCl, Zn_2CrCl, Zn_3AlTar, Zn_2CrTar, and $Zn_3AlTSPP$.

was observed for oxoanions containing LDH, moderate thermal treatments lead to a contraction of basal spacings. But such treatments gave prominence not to a grafting but to a reorientation of tartrate or succinate into the interlamellar space at about 343 K. This reorientation endows the phase with stability up to 523 K; this proves that we have strengthened the interactions between organic anions and inorganic host. Similar results were also evidenced for LDH intercalated with hydroxy aromatic carboxylates (a publication is in preparation).

Acknowledgment. We thank Mr. J. Inacio, a junior researcher, for recording N_2 adsorption−desorption isotherms on some hybrid LDH phases.

IC9801239